Biointerface Research in Applied Chemistry
Platinum Open Access Journal (ISSN: 2069-5837)

Article
Volume 11, Issue 6, 2021, 14078 - 14089
https://doi.org/10.33263/BRIAC116.1407814089

A new Approach on Electrochemical Properties of Poly Aniline and Polymer Binders Impregnated Zn/ZnO Powders as Anodic Electrodes for Energy Storage Devices

Dinakaran Rajamani [1], **Karthikeyan Sambantham** [2,*]

[1] Department of Mechanical Engineering, Pondicherry Engineering College, Puducherry, India
[2] School of Advanced Sciences, Vellore Institute of Technology, Vellore, Tamilnadu, India
* Correspondence: skarthikeyanphd@vit.ac.in;

Scopus Author ID 55516432800

Received: 23.01.2021; Revised: 2.03.2021; Accepted: 4.03.2021; Published: 6.03.2021

Abstract: A novel battery consisted of Zn/ZnO anode with polymer binders has been developed by the direct mixing method. The influence of PANI on the performances of Zn/ZnO anode surfaces has been studied using cyclic voltammetry, Tafel polarization, and Impedance studies. The additions of PANI have not formed any coatings on Zn/ZnO anodes. However, a thin layer of PANI has formed. XRD studies revealed that influence of PANI on the Zn/ZnO anodes had not shown any significant changes in the hexagonal phase. SEM images confirmed that Zn's dendrite structure is prevented by polymers such as PVP, PVA, and microemulsion of castor oil. The impedance studies have demonstrated that there is a reduction in Rct values accounted for enhanced conductance of Zn/ZnO anodes.

Keywords: zinc-zinc oxide anode material; polymer; SEM; XRD; polarization; impedance.

1. Introduction

A variety of energy supplies of humankind had been for a long time met by fossil fuels such as oil, coal, natural gas, and biomass. Although, in modern times, the total availability of fossil fuels and the identification of unsympathetic critical effects such as global warming and pollution on the environment coupled with the depletion of fossil fuel reserve, price acceleration, and various additional riskiness's have led to emerging technologies based on alternative reusable sources of energy. Energy resources such as solar energy, wind energy, hydro and geothermal energy have been recognized as potential sources for the harness of clean and green energy [1]. These resources have a sequential and spatial dependence, andit's required a specific place to store the energy [2]. Devices used for storing the electrochemical energy and conversion consisted of batteries, supercapacitors, and fuel cells.

Xinming Fan *et al*. reported that the combination of ZnO and CeO_2 to Ni-Zn rechargeable battery improved electrochemical performance [3-5]. Initially, John Frederic Daniell (British chemist) developed the Daniell cell in the year 1836, the main rational power source, whirl intent in an industry, and a powerhouse of broadcast systems for electrical energy. Generally, it consisted of a container made up of copper filled with a solution of $CuSO_4$, which was immersed in sulfuric acid, and an electrode made up of zinc [6]. The above-saturated cell uses electrolytes, which are disposed to fall out if concerned efficiency has not been achieved.

In the 19th century, batteries' development consisted of the cell that was dry; the aqueous electrolyte was replaced by a paste, completed compacted devices for storing

electricity [7]. Due to intense applications of electronic, compact, and telecommunication devices, researchers significantly concentrated on developing rechargeable batteries with higher electrochemical performances wherein chemistry plays a major role in the development [8-10]. The electric conductivities of an organic-inorganic polymer are less toxic, safer and hence recently, researchers focused on the solid-state electrolytes involving the polymer as an anode or cathode electrodes to develop the metal oxide-polymeric rechargeable batteries for energy storage applications. The corrosion protection, better electrochemical properties, thermal stability, and low cost of polymeric batteries are good. It was reported that [11-15] the higher conductivity, environmental stability, and redox reversibility of polyaniline(PANI) electrode in energy storage devices deserved much consideration in recent years. A few unique mix substances of electrode and electrolyte were utilized, including Ni-Cd, Pb-acid, Ni-MH, Li-ion, and Li-ion polymer. Bai *et al*. employed ZnO@C nono spheres as an anode material for Li-ion batteries and studied the electrochemical performances [16-17].

A Ni-Zn battery had a discharge voltage of 1.6 V for up to 200 cycles; after that, failure occurs due to dendrite growth, leading to cell shortening and shape changes [18]. Ke Wang *et al*. demonstrated that the flower-like Zn_2SnO_4 composites for the lithium-ion anode batteries had 501 $mAhg^{-1}$ higher reversible capacity after 50 cycles of performance [19].

The addition of alloying elements to the anode or cathode would suppress the shape change and dendrite growth. Jianhang Huang *et al*. [20] synthesized an ultrasound-assisted ZnO/polypyrrole electrode for Ni/Zn rechargeable batteries and reported superior capacity and stable cycle performances. Many researchers have focused on controlling the dendrite growth, shape change, and improved the battery life cycle. Xiayin Yao *et al*. [21] developed a carbon-coated Zinc ferrite nanorods PVA doped polymerization for Li-Ion battery and showed rate capability of 504 and 805 mAh/g at current densities of 2 and 0.5 A/g. The role of metal oxide had a dominant role in developing and improving the batteries' electrochemical performance in recent years. Some additives like $Ca(OH)_2$, BaO, In_2O_3, Bi_2O_3, SnO_2, TiO_2, ZnO, Pb_3O_4, [22]] used to enhance the performance of the Li, Ni-Zinc batteries. The ZnO has more advantages than the other metal oxide due to the existence of larger surface porosity. The addition of bismuth oxide to the Ni-Zn-based ZnO/KOH electrolyte resulted in no agglomeration was noticed with other particles in the composite used in the battery [23]. Uniform Carbon-plated ZnO anode material for Nickel-Zinc battery had good corrosion resistance and cycle performances [20]. Metal oxide also played a vital role in developing anode material for a Li-ion battery and increasing the specific capacity besides cycle efficiency, e.g., $ZnSnO_3$-C, ZnO/rGO, $Li_4Ti_5O_{12}$, $ZnFe_2O_4$/C, MWCNT reinforced ZnO, $Zn_{0.5}Ni_{0.5}Co_2O_4$, $ZnMn_2O_4$/C, ZnO/Ni/C [24-35]. Based on the above literature reports, it is imperative to develop zinc anode which should possess the characteristic such as zinc mobility retardation, shape change, and lower densification are to have arrived. Also, the deterring dendrites formation along with zinc mobility retardation overcomes the certain failure of other batteries. This has been achieved as follows: In this paper, we have attempted that instead of Zn metal's electrodeposition by Ag/Au, zinc in powder form has been taken. This is mixed with ZnO powders. The particles have an average size of 3 microns for zinc and 5 microns for ZnO (as measured by Fischer- sub-sieve sizer) and having a pore diameter in the range of 4-6 microns. The zinc is preferably loaded into the ZnO pores, taking advantage of ZnO's high surface area, which can impregnate Zn powder. Also, the addition of PANI, Activated carbon, PVP, PVA, and microemulsion of castor oil retards the migration of zinc due to the availability of larger pores within the resulting matrix. Thus the cycle life of the battery is increased. However, no

significant reports are available on ZnO/Zn energy storage systems' performance, which are easy to manipulate, assemble, and inexpensive. The present research paper involves the development of a novel Metal-Metal oxide anode for a battery as an alternate to Li and Ni-MH batteries. The present battery contains Zn/ZnO as rechargeable anodic batteries. The stability of zinc electrodes for their usage in prolonged life, metal oxides the later is inert in nature, were employed and binders and electrolytes of the present battery system. The separator was polysiloxanes. The Zn/ZnO anodes' performances have been assessed by electrochemical polarization studies, cyclic voltammetry, and impedance measurements. The formation of dendrite growth of zinc and uniform dispersion zinc in the polymer matrix has been studied by XRD and SEM-EDAX measurements. The results are presented and discussed.

2. Materials and Methods

2.1. Preparation of Zn/ZnO-based electrode.

The Zn/ZnO based anode electrode was prepared as slurries made of A.R. grade chemicals containing Zn metal powder, Zinc oxide pure, Activated carbon, conducting polymer (PANI), binders of Polyvinylpyrrolidone K-30 $((C_6H_9NO)_X,$ and Polyvinylalcohol LR $((C_2H_4O)_n$, were dissolved in 50ml of deionized water under constant mechanical stirring for 30 min. The slurry of ZnO was prepared by mixing with 1M KOH and was used as the electrolyte. Afterward, the mixed slurries were put into an acrylic container (14mm diameter and 25mm height); a casing is shown in fig.1. The composition of Zn/ZnO-based anode electrodes is shown in table 1.

2.2. Material characterization.

The additives added Zn/ZnO particles and plain Zn/ZnO had been characterized by X-ray diffraction analysis (Bruker, Germany, Model: D8 advance Source: 2.2KW Cu-anode ceramic tube) at 30 kV and 40 mA. The additives' morphologies added Zn/ZnO powders and pure Zn, ZnO, were observed by scanning electron microscope (ZEISS EVO15). The elemental analysis of the surface has been measured by Energy Dispersive X-Ray Analysis (EDAX ZEISS EVO15).

2.3. The electrochemical performance measurements.

A three-electrode cell setup was employed for cyclic voltammetry (CV), Tafel plot, and Impedance spectroscopy. The reference electrode was Hg/HgO/1M KOH was used. Platinum of 10 cm^2 was used as the counter electrode and activated Zn/ZnO was used as the working electrode. Cyclic voltammetry was performed with an electrochemical workstation (IVIUM v54800, The Netherlands) a scanning rate was 10 mVs^{-1} and temperature was 28 ± 1° C. Electrochemical impedance spectroscopy performance was carried out using an electrochemical workstation (IVIUM v54800, The Netherlands) with an applied frequency range of 0.1Hz and 100 kHz. Tafel plot was plotted at a scanning rate of 10 mVs^{-1} using the above electrochemical workstation.

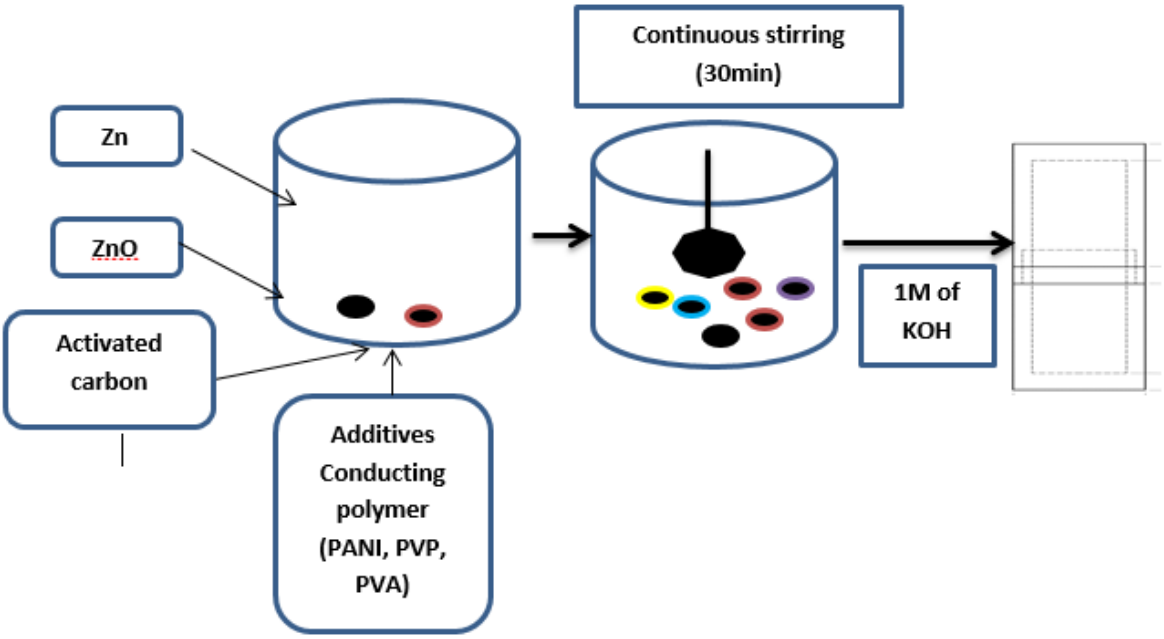

Figure 1. Schematic representation of anode preparation.

Table 1. Composition of Zn/ZnO-based anode electrodes.

Sample No.	Compositions of electrode
	(A) Without PANI
A1	Zn 28.40%, ZnO 68.18%, AC 3.40%
A2	Zn 27.47%, ZnO 65.93%, AC 3.29% , PVP 3.29%
A3	Zn 27.47%, ZnO 65.93%, AC 3.29%, PVA 3.29%
A4	Zn 27.47%, ZnO 65.93%, AC 3.29%, Castor oil 3.29%
	(B) With PANI
A5	Zn 27.47%, ZnO 65.93%, AC 3.29%, PANI 3.29%
A6	Zn 27.47%, ZnO 65.93%, AC 3.29%, PVP 1.64%, PANI 1.64%
A7	Zn 27.47%, ZnO 65.93%, AC 3.29%, PVA 1.64%, PANI 1.64%
A8	Zn 27.47%, ZnO 65.93%, AC 3.29%, Castor oil 1.64%, PANI 1.64%

3. Results and Discussion

3.1. The X-ray diffraction pattern analysis of as-prepared Zn/ZnO electrode.

Figure 2(a) and 2(b) shows that XRD pattern of Zn/ZnO anode in the presence and absence of PANI. The higher sharp peak showed that the anode comprised of ZnO (101) and (002) plane indicated the presence of activated carbon.

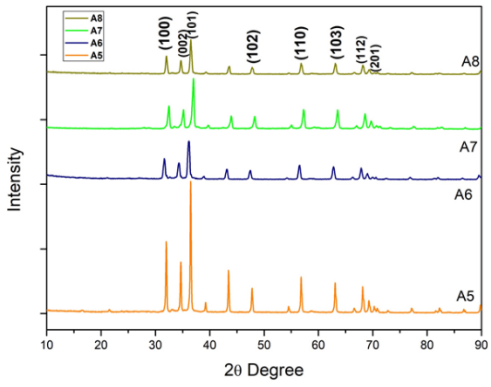

Figure 2(a). XRD pattern without Influence PANI.

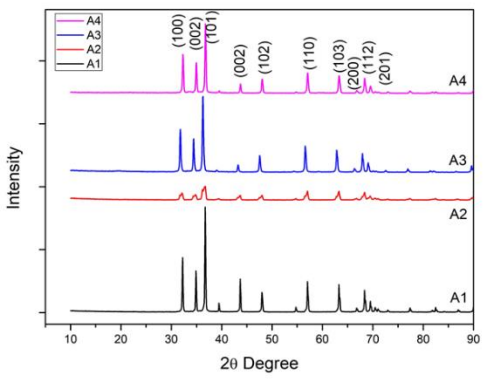

Figure 2(b). XRD pattern with Influence of PANI.

All peaks were sharp, crystalline, and hexagonal phases with the primitive lattice of cell parameters has a = 3.249 Å and c = 5.206 Å. After the inclusion PANI to Zn/ZnO samples, the diffraction peak position and crystalline phase remained the same, and all were matched with the PDF No: 36-1451.

3.2. The scanning electron microscope and EDAX analysis of as-prepared Zn/ZnO electrodes.

SEM images for Zn/ZnO anode are shown in fig. 3 (a) and (b). The image corresponding to sample A1 indicated the presence of the dendrite structure of Zn active material, which is further redistributed in the matrix in the absence of polyaniline. The appearance of gathered sea plant structure indicated in the presence of ZnO. Which got trapped inside the dendrite structure of zinc, and hence the former has shown a decrease in its mobility during discharge. A similar observation has been made in U.S. Pattern [32]. The appearance of the grey layer confirmed the existence of activated carbon. The figure corresponds to sample A2 indicated the agglomeration of PVP atoms in the matrix. The formation of an aloe vera-like structure established the presence of PVA in sample A3. It is evident that the anode is prone to shape change and dendrite short-circuiting when discharging and charging. It was further observed that the dendrite structure's growth induces battery failure, and hence the anode with more life and should apply constant energy had attracted the formulation of sample A4. The SEM images of sample A4 showed that insoluble structure, which effectively tides up the zincate ion, further reduced its diffusion to prevent the battery's failure. In SEM image A4, the formation of uniform dispersed particles of castor oil that enveloped Zn, ZnO, Activated carbon effectively are visible.

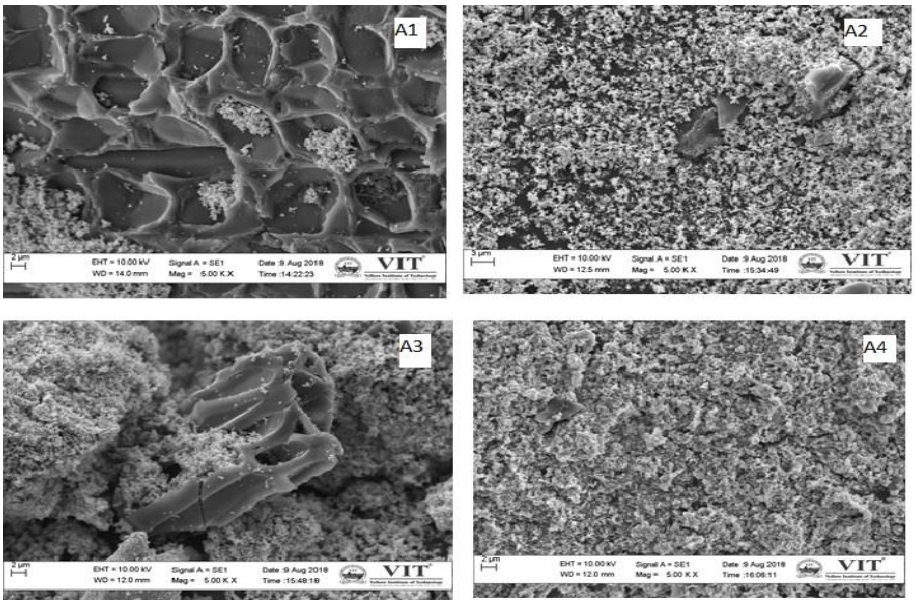

Figure 3(a). SEM micrographs without PANI.

The appearance of a layered structure confirmed the absence of dendrite in figure 3(b) for sample A5 in the presence of PANI, which has a highly flexible structure to release the mechanical strain resulting from the volume change of active material while doping and undoping as observed by Yang. Xia *et al*. [29]. The SEM image of sample A6 in figure 3(b) indicated compatibility in the active material, which might be due to PVP and PANI atomic particles' collision. In sample A7 the SEM image signified that the formation of an aloe vera-like structure further justified the presence of PVA. The addition of castor oil (sample A8)

contributed to the entrapment of PANI, PVP, PVA, which is clearly established through the submerging aloe vera-like structure in the active materials. Fig 3(b) b shows EDAX spectra of as developed Zn/ZnO anode. Zn, C, and O peaks are found in the spectra, which were the surface elemental compositions of Zn/ZnO as prepared. A similar observation was investigated by Dinakaran and Karthikeyan during the intercalation of Graphene/MWCNT as reinforcement particles in Al- Aluminium oxide primary cells [36].

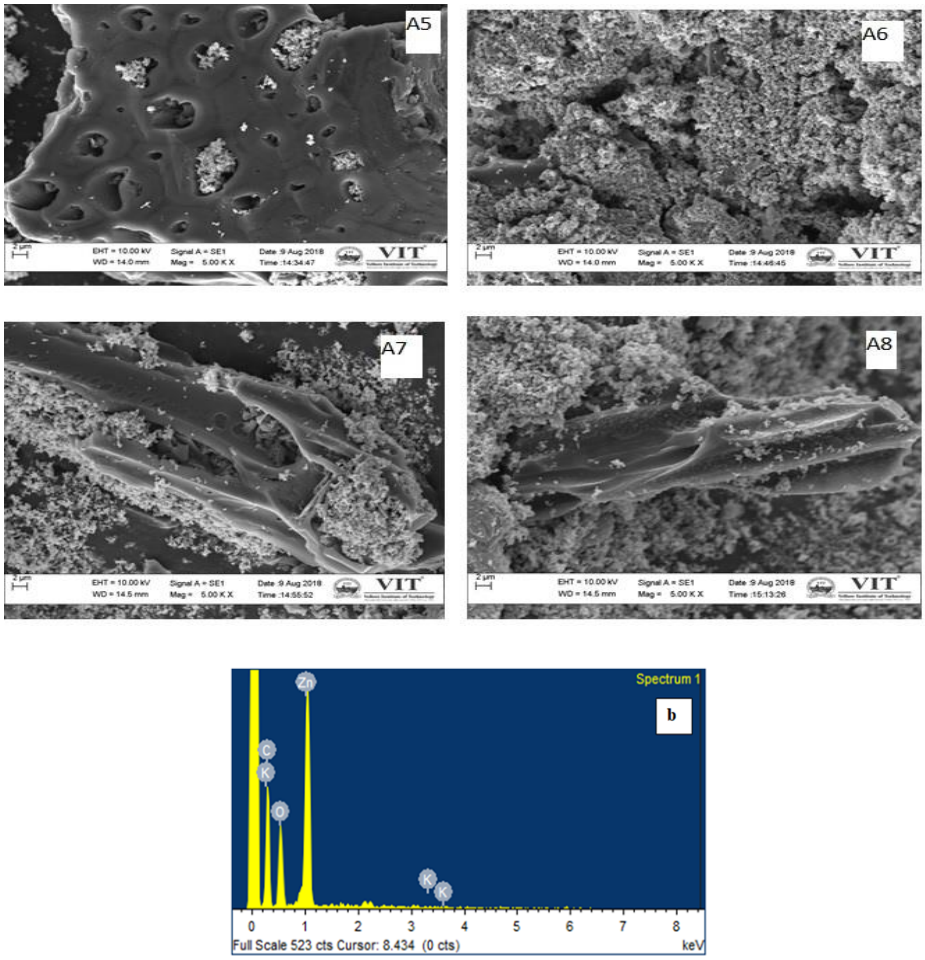

Figure 3(b). SEM Micrographs with PANI sample (A5-A8) and The EDAX spectra of as-prepared Zn/ZnO electrodes.

3.3. Electrochemical properties.

3.3.1. Cyclic voltammetry analysis of Zn/ZnO anode electrodes.

The cyclic voltammetry of the sample with PANI and sample without the influence of PANI is shown in Figure 4(a) and (b). The peak potential for sample A1 is found to be -2.116 V, and the corresponding peak current is 3.08 x 10-6 A. This value confirms the oxidation of Zn/ZnO to a greater extent along with enhancement of peak current values. The peak current for sample A2 is -1.13 V, and the peak current is 0.158 µA. The addition of PVP has controlled the oxidation of Zn/ZnO from -2.116 V to -1.13 V and the corresponding reduction. The cyclic voltammetry of sample A3, PVA gave no significant peak potential and peak current. Due to the fact, the addition of PVA showed little impact on the electrochemical stability within the potential window in the range of 0.17 V to 0.18 V, which are suitable for practical applications in Ni-Mh batteries as reported earlier [32,37].

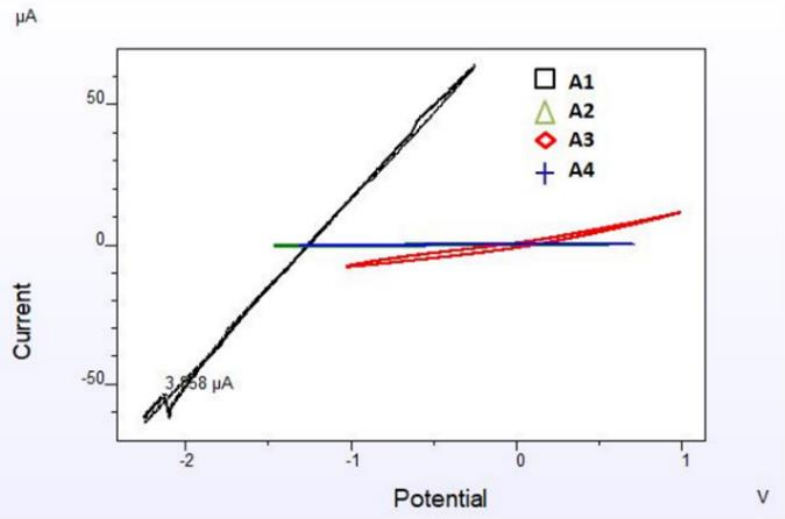

Figure 4(a). The cyclic voltammetry of Zn/ZnO electrodes without PANI.

The addition of castor oil has not changed the electrochemical stability window of PVA-based battery content, but the potential has reduced to 0.144 V, indicating that the addition of castor oil has not favored the reduction of zinc.

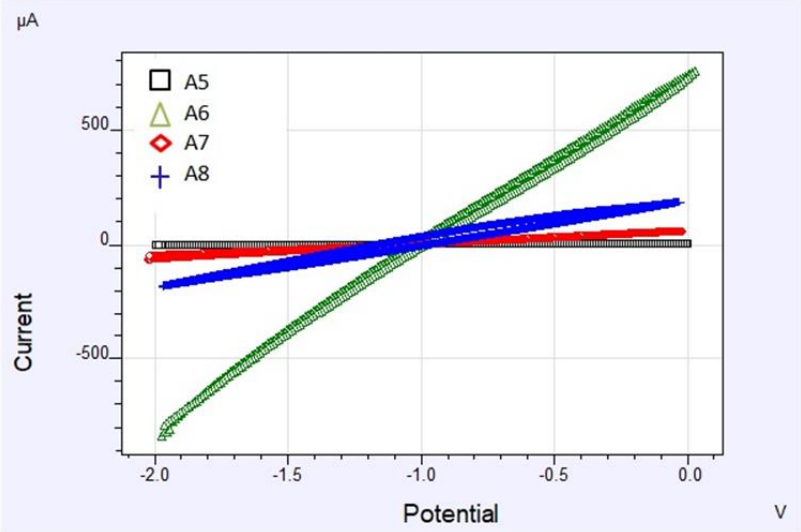

Figure 4(b). The cyclic voltammetry of Zn/ZnO electrodes with PANI.

The cyclic voltammograms of Zn/ZnO supported PANI were recorded in the solution of 10 % KOH. It is evident from figure 4(b) sample A5 to A8 that no clear peak is visualized for the Zn/ZnO anodes, which PANI further supported. The results showed that it is a peculiar property of non-faradic capacitance; also, there is no formation of the electrophoretic coating of PANI on Zn/ZnO. It is furthered demonstrated that the presence of 3D porous composite structure, as evidenced from SEM image 3(b) sample A5, confirmed that there are two approaches for charge retention in the battery. The non-faradic capacitance and faradic redox contribute uniform mixing of PANI with Zn/ZnO. According to Y. Xia *et al*. [27], the absence of oxidation and reduction peak potentials and peak currents have confirmed that the electrophoretic layer has not been formed by PANI on active material. However, PANI has helped reduce the mechanical strain from the volume change of active materials; this is why PVP, PVA, and microemulsion of castor oil have been added with active material.

3.3.2. Tafel plot curve analysis of Zn/ZnO anode electrodes.

Zn's mobility is retarded by a matrix made of PVP, PVA, and castor oil microemulsion.

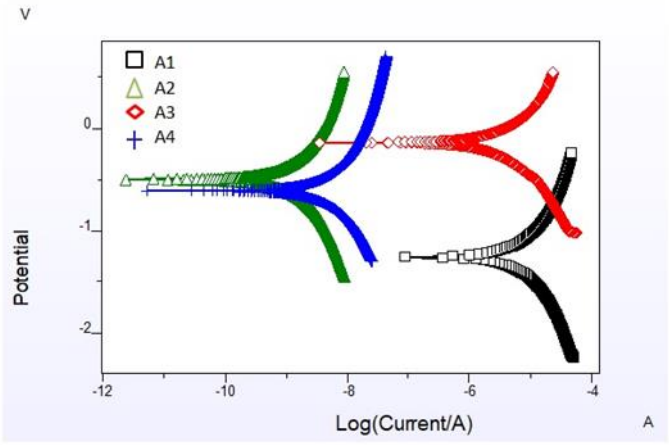

Figure 5(a). The Tafel plot curve of Zn/ZnO electrodes without PANI.

However, the dendrite structure has not been altered due to the existence of a polymer matrix made of PVP and PVA. The results are presented in Figures 5(a) and (b). It is evident that the addition of PVA could significantly retard both E_{corr} and I_{corr} values better than the rest. The anodic reaction is explained as follows:

a) The migration of Zn is reduced, and hence the mobility is prevented.

b) The presence of ZnO micropores entraps a Zn particle that enhances constant current and potential values during discharge.

c) The presence of polymer matrices such as PVP, PVA, and a microemulsion of castor oil reduces the dendrite formation of Zn, which is demonstrated through the shift of Ecorr values to a positive direction, i.e., for Zn/ZnO, Ecorr = -1.2571 V vs. saturated Hg/HgO/1M KOH.

The addition of PVP sample A2 showed E_{corr} values -0.5165 V, and its correspond I_{corr} values is 1.617E-9 A/cm^2. Among the polymer used, PVA sample A3 has performed well, evidenced by the reduction of I_{corr} values of 1.086E-9 A/cm^2. The addition of microemulsion of castor oil has reduced the I_{corr} values but lesser than the PVP. The absence of PVP, PVA, and a microemulsion of castor oil could have made Zn's migration due to gravity. With migration, it would have intensified the accumulation of Zn in ZnO/Activated carbon matrix and hence enhanced polarization [6,36].

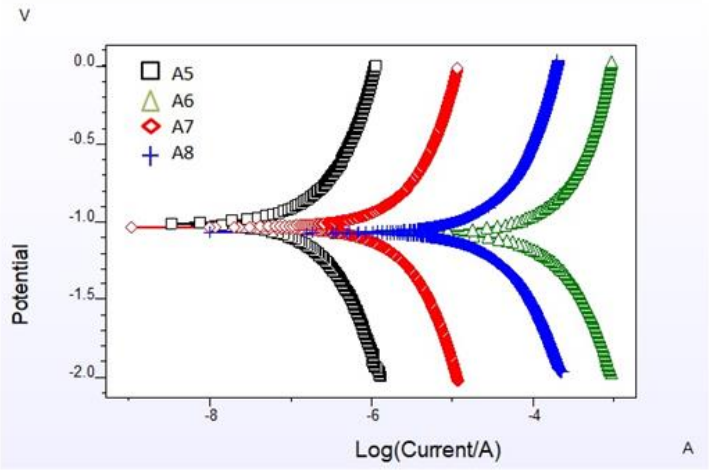

Figure 5(b). The Tafel plot curve of Zn/ZnO electrodes with PANI.

The addition of PANI (ranges from 1.64 % to 3.29 %) had influenced the shift of polarization current of Zn/ZnO anode battery as follows. The mixing of PANI with Zn/ZnO first forms a very thin layer by electrophoresis, which is then stabilized. The presence of PVP and PVA had shifted I_{corr} values to the positive direction indicating the hindrance of dendrite formation of Zn, $E_{corr,}$ and I_{corr} values are shown in table 2. The I_{corr} values for microemulsion of castor oil are 3.277 E-5 A/cm^{2,} which is slightly positive than I_{corr} values of PVA and PVP. This could be accounted for weaker resistance of microemulsion for Zn's migration; the results are given in figure 5(b). The same type of observation was reported by Dinakaran and Karthikeyan for their studies on the corrosion properties of Cu/CuO and Sn/SnO batteries [37].

Table 2 The Tafel plot data for Zn/ZnO electrode with and without the influence of PANI.

Sample	E_{corr} (V)	I_{corr} (A/cm^2)
(A) Without PANI		
A1	-1.2571	8.519E-6
A2	-0.5165	1.617E-9
A3	-0.1346	1.086E-9
A4	-0.5867	1.875E-9
(B) With PANI		
A5	-1.0119	6.022E-5
A6	-1.0928	5.034E-5
A7	-1.0493	2.018E-6
A8	-1.1017	3.277E-5

3.3.3. The electrochemical Impedance spectroscopes of Zn/ZnO anode electrodes.

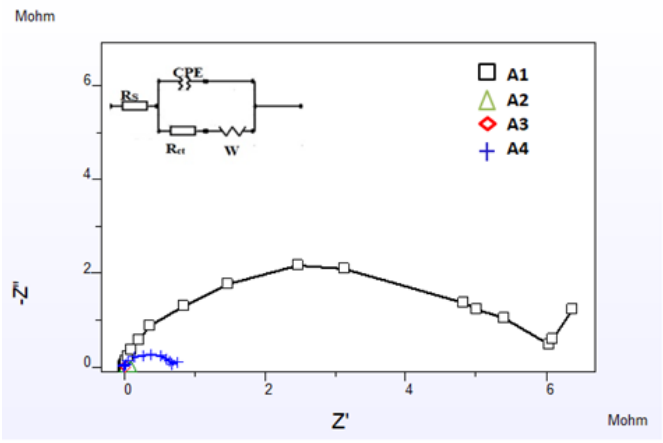

Figure 6(a). The Nyquist plots of Zn/ZnO electrodes without PANI.

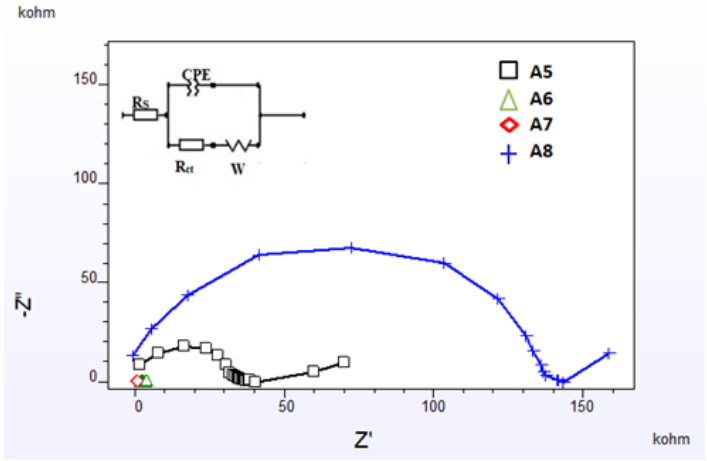

Figure 6(b). The Nyquist plots of Zn/ZnO electrodes with PANI.

To understand the effect of PVP, PVA, and microemulsion of castor oil in the presence and absence of PANI, electrochemical impedance studies were conducted after the 100th discharge of Zn/ZnO anode batteries. The equivalent circuit is incorporated in Figures 6 (a) and (b). It has been noted that a drag semicircle has been obtained due to ohmic resistance with a combination of electrical contact resistance, the conductivity of Zn, and ionic conductivity of PVP, PVA, and microemulsion of castor oil. The charge transfer resistance and double-layer capacitance are the parameters important to us. Since the powders are porous constant phase element (CPE) is introduced along with the total ohmic resistance (R_s), R_{ct} is the charge transfer resistance. The fitted equivalent circuit has resistance due to Warburg (W) impedance. The smaller Rct values indicate a better electrical conductivity. This can be demonstrated through Zn's distribution is more homogeneous in PVP and PVA than activated carbon and microemulsion of castor oil, as shown in table 3. The surface area of Zn is enhanced in the polymer matrix. The Nyquist plots are presented in fig 6 (a) and (b).

Table 3. The data for the impedance spectra for Zn/ZnO electrode with and without the influence of PANI.

Sample	R_{ct} (Ohm)	C_{dl} (µF.cm^{-2})
(A) Without PANI		
A1	5731000	1.569E-10
A2	87730	3.099E-10
A3	11840	4.251E-10
A4	727500	1.230E-10
(B) with PANI		
A5	35660	1.823E-10
A6	2586	1.094E-9
A7	779.5	2.027E-9
A8	138000	1.098E-10

4. Conclusions

The Zn/ZnO-based anode electrodes were prepared by slurries containing Zn metal powder, ZnO pure, and activated carbon. Also, polymers like PVP, PVA, castor oil emulsions have been added as binders, and the results are compared without and with the influence of PANI. XRD result exhibits all peaks are in sharp, crystalline structure and hexagonal phase. SEM micrographs clearly show that influence of PANI reduces the dendrite structure and forms an aloe vera structure. The improvement in cyclic voltammetry shows that the addition of PVP has controlled the oxidation of Zn/ZnO from -2.116 V to -1.13 V along with the corresponding reduction. The mixing of PANI showed that it is a peculiar property of non-faradic capacitance also, there is no formation of the electrophoretic coating of PANI on Zn/ZnO but is limited to a layer formation. However, PANI has helped reduce the mechanical strain from the volume change of active materials to a smaller extent. This is why PVP, PVA, and microemulsion of castor oil have been added with active material. The presence of polymer matrices such as PVP, PVA, and a microemulsion of castor oil hindrance to Zn's dendrite formation proves that the shift of Ecorr and Icorr values to positive direction with and without influence of PANI and also the migration of Zn is reduced. Smaller charge transfer resistance (Rct) was achieved in PVP and PVA than activated carbon and microemulsion of castor oil in the presence and absence of PANI. Among the polymer binder, added PVA exhibited better electrochemical performance.

Funding

This research received no external funding.

Acknowledgments

This research has no acknowledgment.

Conflicts of Interest

The authors declare no conflict of interest.

References

1. Fan, X.; Yang, Z.; Xie, X.; Long, W.; Wang, R.; Hou, Z. The electrochemical behaviors of Zn–Al–La-hydrotalcite in Zn–Ni secondary cells. *Journal of Power Sources* **2013,** *241*, 404–409, https://doi.org/10.1016/j.jpowsour.2013.04.136.
2. Zeng, D.Q.; Yang, Z.H.; Wang, S.W. Preparation and electrochemical performance of In-doped ZnO as anode material for Ni–Zn secondary cells. *Electrochimica Acta* **2011**, *56*, 4075–4080, https://doi.org/10.1016/j.electacta.2011.01.119.
3. Fan, X.; Yang, Z.; Long, W.; Yang, B.; Jing, J.; Wang, R. The preparation and electrochemical performances of the composite materials of CeO2 and ZnO as anode material for Ni–Zn secondary batteries. *Electrochimica Acta* **2013**, *108*, 741-748, https://doi.org/10.1016/j.electacta.2013.07.031.
4. Moser, F.; Fourgeot, F.; Rouget, R.; Crosnier, O.; Brousse, T. In situ X-ray diffraction investigation of zinc based electrode in Ni–Zn secondary batteries. *Electrochimica Acta* **2013**, *109*, 110-116, https://doi.org/10.1016/j.electacta.2013.07.023.
5. Long, W.; Yang, Z.; Fan, X.; Yang, B.; Zhao, Z.; Jing, J. The effects of carbon coating on the electrochemical performances of ZnO in Ni–Zn secondary batteries. *Electrochimica Acta* **2013**, *105*, 40-46, https://doi.org/10.1016/j.electacta.2013.04.162.
6. Xie, Q.; Ma, Y.; Zhang, X.; Guo, H.; Lu, A.; Wang, L.; Yue, G.; Peng, D.-L. Synthesis of amorphous ZnSnO3-C hollow microcubes as advanced anode materials for lithium ion batteries. *Electrochimica Acta* **2014**, *141*, 374-383, https://doi.org/10.1016/j.electacta.2014.07.095.
7. Wu, J.; Chen, C.; Hao, Y.; Wang, C. Enhanced electrochemical performance of nanosheet ZnO/reduced graphene oxide composites as anode for lithium-ion batteries. *Colloids and Surfaces A: Physicochemical and Engineering Aspects* **2015**, *468*, 17-21, https://doi.org/10.1016/j.colsurfa.2014.12.009.
8. Han, C.; He, Y.-B.; Li, H.; Li, B.; Du, H.; Qin, X.; Kang, F. Suppression of interfacial reactions between Li4Ti5O12 electrode and electrolyte solution via zinc oxide coating. *Electrochimica Acta* **2015**, *157*, 266-273, https://doi.org/10.1016/j.electacta.2014.12.080.
9. Yao, L.; Hou, X.; Hu, S.; Wang, J.; Li, M.; Su, C.; Tade, M.O.; Shao, Z.; Liu, X. Green synthesis of mesoporous ZnFe2O4/C composite microspheres as superior anode materials for lithium-ion batteries. *Journal of Power Sources* **2014**, *258*, 305-313, https://doi.org/10.1016/j.jpowsour.2014.02.055.
10. Guler, M.O.; Cetinkaya, T.; Tocoglu, U.; Akbulut, H. Electrochemical performance of MWCNT reinforced ZnO anodes for Li-ion batteries. *Microelectronic Engineering* **2014**, *118*, 54-60, https://doi.org/10.1016/j.mee.2013.12.029.
11. Song, X.; Ru, Q.; Mo, Y.; Guo, L.; Hu, S.; An, B. A novel porous coral-like Zn0.5Ni0.5Co2O4 as an anode material for lithium ion batteries with excellent rate performance. *Journal of Power Sources* **2014**, *269*, 795-803, https://doi.org/10.1016/j.jpowsour.2014.07.077.
12. Alfaruqi, M.H.; Rai, A.K.; Mathew, V.; Jo, J.; Kim, J. Pyro-Synthesis of Nanostructured Spinel ZnMn2O4/C as Negative Electrode for Rechargeable Lithium-Ion Batteries. *Electrochimica Acta* **2015**, *151*, 558-564, https://doi.org/10.1016/j.electacta.2014.11.066.
13. Xie, Q.; Ma, Y.; Zhang, X.; Wang, L.; Yue, G.; Peng, D.-L. ZnO/Ni/C composite hollow microspheres as anode materials for lithium ion batteries. *Journal of Alloys and Compounds* **2015**, *619*, 235-239, https://doi.org/10.1016/j.jallcom.2014.08.240.
14. Li, Z.; Gong, L. Research Progress on Applications of Polyaniline (PANI) for Electrochemical Energy Storage and Conversion. *Materials* **2020**, *13*, 548. https://doi.org/10.3390/ma13030548.
15. Forouzandeh, P.; Kumaravel, V.; Pillai, S.C. Electrode Materials for Supercapacitors: A Review of Recent Advances. *Catalysts* **2020**, *10*, 969. https://doi.org/10.3390/catal10090969.
16. Jayaraman, T.; Salla, Sunitha.; Senthil.; Palaniyandy, N.; Kumar, M.; Arunachalam, P.; Maiyalagan, T.; Kim, H-S. A Review on ZnO Nanostructured Materials: Energy, Environmental and Biological Applications. *Nanotechnology* **2019**, *30*, https://doi.org/10.1088/1361-6528/ab268a.

17. Bai, Z.; Zhang, Y.; Fan, N.; Guo, C.; Tang, B. One-step synthesis of ZnO@C nanospheres and their enhanced performance for lithium-ion batteries. *Materials Letters* **2014**, *119*, 16-19, https://doi.org/10.1016/j.matlet.2013.12.060.
18. Huang, X.H.; Xia, X.H.; Yuan, Y.F.; Zhou, F. Porous ZnO nanosheets grown on copper substrates as anodes for lithium ion batteries. *Electrochimica Acta* **2011**, *56*, 4960-4965, https://doi.org/10.1016/j.electacta.2011.03.129.
19. Wang, K.; Huang, Y.; Huang, H.; Zhao, Y.; Qin, X.; Sun, X.; Wang, Y. Hydrothermal synthesis of flower-like Zn2SnO4 composites and their performance as anode materials for lithium-ion batteries. *Ceramics International* **2014**, *40*, 8021-8025, https://doi.org/10.1016/j.ceramint.2013.12.154.
20. Huang, J.; Yang, Z.; Yang, B.; Wang, R.; Wang, T. Ultrasound assisted polymerization for synthesis of ZnO/Polypyrrole composites for zinc/nickel rechargeable battery. *Journal of Power Sources* **2014**, *271*, 143-151, https://doi.org/10.1016/j.jpowsour.2014.07.140.
21. Yao, X.; Kong, J.; Zhao, C.; Zhou, D.; Zhou, R.; Lu, X. Zinc ferrite nanorods coated with polydopamine-derived carbon for high-rate lithium ion batteries. *Electrochimica Acta* **2014**, *146*, 464-471, https://doi.org/10.1016/j.electacta.2014.08.144.
22. Cui, J.; Yang, J.; Man, J.; Li, S.; Yin, J.; Ma, L.; He, W.; Sun, J.; Hu, J. Porous Al/Al_2O_3 two-phase nanonetwork to improve electrochemical properties of porous C/SiO_2 as anode for Li-ion batteries. *Electrochimica Acta* **2019**, 300, 470–481, https://doi: 10.1016/j.electacta.2019.01.121.
23. He, S.; Wei, J.; Guo, F.; Xu, R.; Li, C.; Cui, X.; Zhu, H.; Wang, K.; Wu, D. A large area, flexible polyaniline/buckypaper composite with a core–shell structure for efficient supercapacitors. *Journal of Materials Chemistry A* **2014**, *2*, 5898-5902, https://doi.org/10.1039/C4TA00089G.
24. Wei, J.; Xing, G.; Gao, L.; Suo, H.; He, X.; Zhao, C.; Li, S.; Xing, S. Nickel foam based polypyrrole–Ag composite film: a new route toward stable electrodes for supercapacitors. *New Journal of Chemistry* **2013**, *37*, 337-341, https://doi.org/10.1039/C2NJ40590C.
25. Long, W.; Yang, Z.; Fan, X.; Yang, B.; Zhao, Z.; Jing, J. The effects of carbon coating on the electrochemical performances of ZnO in Ni–Zn secondary batteries. *Electrochimica Acta* **2013**, *105*, 40-46, https://doi.org/10.1016/j.electacta.2013.04.162.
26. Xiang, X.; Liu, E.; Huang, Z.; Shen, H.; Tian, Y.; Xiao, C.; Yang, J.; Mao, Z. Preparation of activated carbon from polyaniline by zinc chloride activation as supercapacitor electrodes. *Journal of Solid State Electrochemistry* **2011**, *15*, 2667-2674, https://doi.org/10.1007/s10008-010-1258-7.
27. Tan, Q.; Kong, Z.; Chen, X.; Zhang, L.; Hu, X.; Mu, M.; Sun, H.; Shao, X.; Guan, X.; Gao, M.; ; Xu, B. Synthesis of SnO_2/graphene composite anode materials for lithium-ion batteries. *Applied Surface Science. Elsevier* **2019** *485*, 314–322, https://doi: 10.1016/j.apsusc.2019.04.225.
28. Shi, Y.; Wen, L.; Pei, S.; Wu, M.; ; Li, F. Choice for graphene as conductive additive for cathode of lithium-ion batteries. *Journal of Energy Chemistry* 2019, *30*, 19–26, https://doi: 10.1016/j.jechem.2018.03.009.
29. Xia, Y.; Zhu, D.; Si, S.; Li, D.; Wu, S. Nickel foam-supported polyaniline cathode prepared with electrophoresis for improvement of rechargeable Zn battery performance. *Journal of Power Sources* **2015**, *283*, 125-131, https://doi.org/10.1016/*j*.jpowsour.2015.02.123.
30. Eqbal, E.; Raphael, R.; Saji, K. J.; Anila, E. I. Fabrication of p-SnO/n-SnO_2 transparent p-n junction diode by spray pyrolysis and extraction of device's intrinsic parameters. *Materials Letters*. *Elsevier* **2019,** *247*, 211–214, https://doi: 10.1016/j.matlet.2019.03.122.
31. Yin, W.; Chai, W.; Wang, K.; Ye, W.; Rui, Y.; Tang, B. Facile synthesis of Sb nanoparticles anchored on reduced graphene oxides as excellent anode materials for lithium-ion batteries. *Journal of Alloys and Compounds* **2019**, 1249-1257, https://doi: 10.1016/j.jallcom.2019.04.329.
32. Allen, C.; Brookfield.; Dwaine, K.; Coates, D. Calcium-Zincate electrode for alkaline batteries and method for making same. U.S. Pattern. 5863676. **1997.**
33. Fan, L.; Wang, M.; Zhang, Z.; Qin, G.; Hu, X.; Chen, Q. Preparation and Characterization of PVA Alkaline Solid Polymer Electrolyte with Addition of Bamboo Charcoal. *Materials* **2018,** *11*, https://doi.org/10.3390/ma11050679.
34. Arun, T.; Prabakaran, K.; Udayabhaskar, R.; Mangalaraja, R. V.; Akbari-Fakhrabadi, A. Carbon decorated octahedral shaped Fe_3O_4 and α-Fe_2O_3 magnetic hybrid nanomaterials for next generation supercapacitor applications. *Applied Surface Science. Elsevier* **2019** *485*, 147–157, https://doi: 10.1016/j.apsusc.2019.04.177.
35. Sun, L.; Si, H.; Zhang, Yuanxing, Shi, Y.; Wang, K.; Liu, J.; Zhang, Yihe. Sn-SnO_2 hybrid nanoclusters embedded in carbon nanotubes with enhanced electrochemical performance for advanced lithium ion batteries. *Journal of Power Sources. Elsevier* **2019**, *41*, 126–135, https://doi: 10.1016/j.jpowsour.2019.01.063.
36. Dinakaran, R.; Karthikeyan, S. Studies on intercalation of graphene and MWCNT as reinforcement particles in Al/Al2O3-based primary cells. *Ceramics International* **2020**, *46*, 12499-12506, https://doi.org/10.1016/j.ceramint.2020.02.012.
37. Dinakaran, R.; Karthikeyan, S. An experimental approach on Cu/CuO-Sn/SnO with graphene/MWCNT composites as a novel primary cell with an extended life span. *Materials Research Express* **2019**, *6*, https://doi.org/10.1088/2053-1591/ab4ca6.